

An Open-Source OpenSim Oculomotor Model for Kinematic and Dynamic Simulation

Constantinos Filip, Dimitar Stanev¹ and Konstantinos Moustakas

July 9, 2018

¹Electrical and Computer Engineering Department, University of Patras, Greece, Corresponding author: stanev@ece.upatras.gr

Abstract

bla

Introduction

Rapid and accurate eye movements are crucial for coordinated direction of gaze. Studying human eye movement has significant implications for improving our understanding of the oculomotor system and treating visuomotor disorders. Over the years, biomechanic simulation has provided an analysis tool of different human movements, especially gait. This analysis can be extended to visual tasks by analyzing the mechanisms of ocular motility and providing a realistic ocular model that can be used to investigate muscle activation patterns during static fixations and the control and dynamics of various eye movements. This model can be used to calculate metabolic costs of eye movements and also simulate different eye disorders, such as different forms of strabismus. Furthermore, it can be easily integrated into other human body models to analyze the relation between vestibular system and eye movement by simulating their biomechanics in three dimensions and investigating the function and neural control of the **Extraocular Muscles (EOMs)**.

Eye movements are produced through the activation of six **EOMs**. Clinical trials have provided a profound knowledge of how the **EOMs** rotate the globe, the resistive tension to this rotation and the length-tension relationship of the muscles. Various computational models of the extraocular muscle and orbital mechanics have been proposed, which provide insight and scientific bases for oculomotor biomechanics, control of eye movement and binocular misalignment. These models focus on the realism of muscle behavior and they were based on the viscoelastic properties and physiological data **EOMs**.

The first 3D biomechanical model was developed by **Robinson (1975)**, who simplified the formulation by only considering the elasticity of the **EOMs** and ignoring the dynamics. The model incorporates anatomically realistic muscle paths and empirical innervation-length-tension relationships. To study the neural control of rapid saccadic movement, models using anatomical and mechanical properties of **EOMs** have been developed. They take account that the actual force is a complex nonlinear function of the muscle length, velocity, and innervation **Millard et al. (2013)**. Such models have the advantage of supporting 3D dynamic simulations and have been used to analyze neural controllers and the pulley hypothesis.

Here, we introduce a detailed 3D biomechanical model, based on the work of **Iskander** of the human eye which can be used for dynamic simulation. The model is based on the biomechanical simulator **OpenSim Delp et al. (2007)**. This is an open-source software that can provide the flexibility of in depth parameterization of the model. The architecture and dynamic muscle properties are based on physiological and kinematic measurements of the human eye. The model incorporates an eye-globe, orbital suspension tissues and six muscles with their connective tissues to test the passive pulley hypothesis. Furthermore, with this model we are able to assess the excitation and activation patterns for a variety of targets by applying a closed-loop fixation controller that drives the model to perform saccadic movements in a forward dynamic manner. The controller minimizes the error between the desired trajectory (reference input) and the predicted movement (calculated output).

Methods

Eye Modeling

The orbital plant consists of the globe (eyeball), three pairs of extraocular muscles, and connective tissues. The size of an emmetropic human adult eye is approximately 0.0242 m (transverse, horizontal), 0.0237 m (sagittal, vertical), 0.022–0.0248 m (axial, anteroposterior) with no significant difference between sexes and age groups. In the transverse diameter, the eyeball size may vary from 0.021 m to 0.027 m. Thus, it can be approximated by a solid sphere with 0.012 m radius. The eyeball was constructed in **Blender**, an open-source software 3D creation software. We used a spherical mesh with 32 segments and 12 rings, to construct the vitreous humor (body) as solid sphere and a conical plate to

construct the cornea. The weight of an average human eye is 0.0075 kg and the moment of inertia can be calculated similarly as in the case of a spherical homogeneous and isotropic object with radius 0.012 m ($I = 2/5mr^2$ at the center of mass).

Muscle Modeling

The six **EOMs**, including four rectus muscles and two oblique muscles, are controlled by the cranial nerves so as to track a visual target and to stabilize the image of the object. The **Lateral Rectus (LR)** and **Medial Rectus (MR)** muscles form an antagonistic pair to produce horizontal eye movements. The **Superior Rectus (SR)** and **Inferior Rectus (IR)** muscles form the vertical antagonist pair, which mainly controls vertical eye movement and also affects rotation about the horizontal plane and the line of sight (secondary action) due to insertion positions and the path of the muscles. The **Superior Oblique (SO)** muscle passes through the cartilaginous trochlea attached to the orbital wall, which reflects the **SO** path by 51 deg. The **Inferior Oblique (IO)** muscle originates from the orbital wall anteroinferior to the globe center and inserts on the sclera posterior to the globe equator. The primary actions of **SO** and **IO** cause rotation of the globe around the visual axis and vertical movement.

We have chosen the passive pulley model for our extraocular model in order to keep it simple and provide faster simulation speed. **Table 1** shows the positions of muscle pulleys, as well as the origin and insertions points of the **EOMs** onto the eye, with respect the center of the globe. These data were acquired from **Iskander 2018** which were based on physiological measurements, but in our case, they were slightly modified to be located outside of the globe radius in order to not penetrate the eye globe. Since no position was documented for the origin of the **SO**, a point close to the origins of the rectus muscles was chosen to match the fiber length in the primary position of the **SO** muscle.

Table 1: Muscle path for the six **EOMs** (dimensions are given in meters).

Muscle	Origin			Pulley			Insertion		
	O_x	O_y	O_z	P_x	P_y	P_z	I_x	I_y	I_z
LR	-0.034	0.0006	-0.013	-0.0102	0.0003	0.012	0.0065	0	0.0101
MR	-0.030	0.0006	-0.017	-0.0053	0.00014	-0.0146	0.0088	0	-0.0096
SR	-0.0317	0.0036	-0.016	-0.0092	0.012	-0.002	0.0076	0.0104	0
IR	-0.0317	-0.0024	-0.016	-0.0042	-0.0128	-0.0042	0.00805	-0.0102	0
SO	0.0082	0.0122	-0.0152	-0.030834	0.001145	-0.01644	0.0044	0.011	0.0029
IO	0.0113	-0.0154	-0.0111	-0.00718	-0.0135	0	-0.008	0	0.009

The Millard muscle model **Millard et al. (2013)** has been adopted for the modeling of the **EOMs**, which allows to manually fit force-generation dynamics. The six **EOMs** were modeled using the rigid tendon assumption that ignores the elasticity of the tendon. This means that the series element of the muscle model is not included (the tendon length l^T is equal to the tendon slack length l_s^T). This assumption is valid when the ratio of the tendon length to the muscle length is less or equal to one, as the in the case of all **EOMs**. **EOMs** are considered parallel-fibered muscles, so the pennation angle is zero ($\alpha = 0$). Maximum isometric force f_o^M , optimal fiber length l_o^M and tendon length l^T are presented in **Table 1** and are based on **Iskander 2018**.

The active and passive **Force-Length (F-L)** curves for the **EOMs** differ from the ones that of the skeletal muscles. As shown in **Figure 1** can be adapted so as to fit the experimental data available for the glslr muscle. The following values were used for the active **F-L** curve:

- min norm active fiber length: 0.55
- transition norm fiber length: 0.7

- max norm active fiber length: 1.8
- shallow ascending slope: 2.4
- minimum value: 0.0

and for the passive F-L curve accordingly:

- strain at zero force: -0.18
- strain at one norm force: 0.4

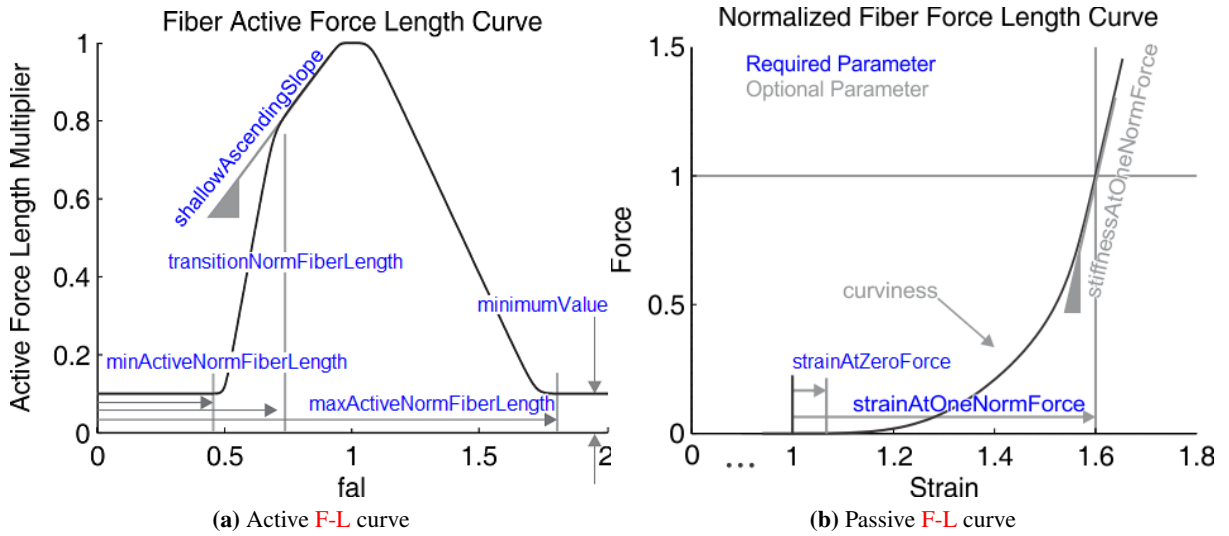


Figure 1: The active and passive F-L curve definition of the Millard muscle model as implemented in OpenSim.

The parameters that describe the above relationships were chosen to fit the curves found in Iskander 2018. In the plots below, we try to match the F-L relationships at maximum activation of the lateral rectus muscle. This represents the first part of testing the fidelity of the model. Due to lack of data describing the other muscles' F-L relationships, we used the parameters found describing the normalized curves of active and passive F-L relationships of the glslr for the other EOMs as well.

EOMs have a higher fraction of fast twitch fibers and thus different Force-Velocity (F-V) behavior, due to different structures compared to skeletal muscles. The default Millard F-V curve was used for the six EOMs, since the behavior of the selected muscle model depends mainly on the maximum contraction velocity v^{\max} . The maximum muscle contraction velocity is tuned so as to match the peak velocity of saccadic eye movement 15.7 rad / s. Following this definition, the maximum muscle contraction velocity is given in optimal fiber length per seconds and it is thus different for each EOMs since their optimal fiber length is different. Also, because of different structure of neural control of eye movements, activation and deactivation delays are lower than in skeletal muscles, at about 5 ms.

Wrapping objects help to simulate the proper dynamics. Using wrapping objects implemented in the OpenSim allows us to model realistic force directions as the muscle runs over the eyeball. From the point of origin to the pulley point, the force exerted by the contraction of the muscles is aligned along one straight line. But, from the pulley point to the insertion point, the force is distributed along the surface of a sphere. Two separate wrapping spheres for the rectus muscles and the oblique muscles were created, to avoid abnormal changes on the F-L curve as the eyeball rotates in the three directions.

Table 2: Millard muscle parameters for the **EOMs**.

Muscle	Maximum Isometric Force (N)	Optimal Fiber Length (m)	Tendon Slack Length (m)	Maximum Contraction Velocity (m / s)
LR	1.4710	0.04898	0.0084	3.8483
MR	1.5740	0.04084	0.0038	4.6155
SR	1.1768	0.04487	0.0054	4.2009
IR	1.4269	0.04549	0.0048	4.1437
SO	0.6031	0.03956	0.0265	4.7648
IO	0.5590	0.04110	0.0015	3.5863

Passive Connective Tissues

The passive connective tissues of the eyeball apply a restoring force, which brings the globe back to the central position when the net force from the **EOMs** is zero. These tissues include all non-muscular suspensory tissues, such as Tenon’s capsule, the optic nerve, the fat pad and the conjunctiva. The force-displacement curve of the net elasticity can be represented as

$$\mathbf{f}_t = -k_p \mathbf{q} - k_c 10^{-3} \mathbf{q}^3 - k_d * \dot{\mathbf{q}} \quad (1)$$

where, \mathbf{f}_t represents the passive tissue forces, $k_p = 0.002225$ N m / rad, $k_c = 34.5297$ N m / (rad³) and $k_v = 0.002$ N m s / rad the constants and $\dot{\mathbf{q}} \in \mathbb{R}^3$ the rotational coordinates of the model. These forces serve the eye’s stabilization, and are modeled using OpenSim’s expression based coordinate force.

Results

Model Validation

To meet good fidelity criteria, a model requires to be verified and validated. In our study, verification in oculomotor models was performed by comparing the **F-L** characteristic curves of the modeled **EOMs** to published data. These data include only the lateral rectus characteristic curves. However, we can make a safe assumption that the other muscles have similar properties. More characteristic curves showing the **F-L** relationship of the other **EOMs**, as well as the changes in muscle length with rotation in all directions, are presented in the end of this report. Further verification can be done by comparing the model’s joint forces produced during horizontal movement with clinically collected data, but these data are not available. Validation was performed by simulating and analyzing synthesized eye movements while ensuring that Listing Law was obeyed by maintaining zero torsion in secondary gaze positions, and by testing if the assessed innervations are sufficient in fixating the eye at a desired position.

Fixation Controller

Conclusion

A realistic ocular model that represents the ocular motility of a normal human eye was presented. The model can be used to simulate different saccadic movements and obtain the muscle activations required to track the movement. The model was validated against experimental measured data and is able to synthesize saccadic movements reasonably well.

We even showed that the simulation results produced by static optimization and forward dynamics in OpenSim are less satisfactory than the proposed solution where we used a **Proportional Derivative**

(PD) controller to minimize the tracking error between the desired and estimated trajectory of saccadic movements. The desired kinematics were tracked within a maximum **Root Mean Square Error (RMSE)** of and in horizontal and vertical saccades respectively. With the application of the controller, a very rapid instantaneous acceleration and a constant velocity to sustain clear vision is attained. The produced activation levels were in accordance with the descriptions found in the bibliography and the highest activation levels were shown only during the time intervals when the main agonist muscle was activated.

Bibliography

- M. Millard, T. Uchida, A. Seth, and S. L. Delp, “Flexing computational muscle: modeling and simulation of musculotendon dynamics,” *Journal of Biomechanical Engineering*, vol. 135, no. 2, pp. 1–12, mar 2013.
- S. L. Delp, F. C. Anderson, A. S. Arnold, P. L. Loan, A. Habib, C. T. John, E. Guendelman, and D. G. Thelen, “OpenSim : Open-Source Software to Create and Analyze Dynamic Simulations of Movement,” *IEEE Transactions on Biomedical Engineering*, vol. 54, no. 11, pp. 1940–1950, 2007.